ISSN 1454 - 8003
Proceedings of 2018 International Conference on Hydraulics and Pneumatics - HERVEX
November 7-9, Băile Govora, Romania

CAD-CAE MODEL FOR THE STRUCTURAL ANALYSIS OF A DRIP TAPE INJECTION EQUIPMENT FOR SUBSURFACE IRRIGATION

Gabriel GHEORGHE[1], Dragoș MANEA[1], Marinela MATEESCU[1], Radu POPA[1], Vlad POPA[1], Gheorghe ȘOVĂIALĂ[2]

[1] National Institute of Research-Development for Machines and Installations Designed to Agriculture and Food Industry INMA Bucharest, Romania, gabrielvalentinghe@yahoo.com

[2] Hydraulics and Pneumatics Research Institute INOE 2000-IHP, Romania, sovaiala.ihp@fluidas.ro

Abstract: *Subsurface drip irrigation is a great irrigation system for field crops. With regard to drip irrigation on the surface, subsurface irrigation offers the possibility of performing all mechanized agricultural work. This system is all the more advantageous as it saturates the root, greatly reduces the risk of weeds, greatly reducing workload. The subsurface drip irrigation system can be installed at various depths, depending on the type of crop crops, germination bed preparation, roots depth. For field crops, the installation depth is 30 ... 40 cm. This article presents the way to obtain the structural model for elementary linear-elastic static analysis of main resistance structure of a drip tape injection equipment. Also, to prove the functionality of the structural model obtained, structural analysis results for the linear elastic static test are presented. These results are useful for estimating the safety factor and for assessing the behaviour in major overstress situations at the main part of the machine*

Keywords*: Structural model, structural analysis, tape injection platform, subsurface drip irrigation*

1. Introduction

Use of subsurface drip irrigation (SDI) has progressed from being a novelty employed by researchers to an accepted method of irrigation of both perennial and annual crops [1]. SDI is a management tool that allows precise control over the root zone environment of the crop. This control often results in consistently high yields. In addition, better water and fertilizer management can help reduce fertilizer inputs, water needs, and runoff. [2] The first step in the installation process of an SDI consists in the drip tape injection. Considering the long-term use of the subsurface drip irrigation system, the dripline must be buried below the plough layer [3]. The injector consists of a roll that holds the tape and a shank that opens the soil to bury the tape [4]. As the shank opens the soil, the tape is guided into the soil, usually through a curved pipe mounted behind the shank. The shank must be durable enough to resist the impact of rocks and other obstructions in the soil. The pipe that is mounted behind the shank should be smooth and curved so it does not tear the tape.

Optimal design or improvement of a complex mechanical structure are activities that are currently carried out in the work of advanced companies working in the field of mechanical and other types structures. Designing an optimal product (at least from some points of view) or optimizing existing products requires complex working tools that are nowadays integrated into CAD-CAE complex programs. The workflow in the CAD - CAE complex is often fragmented, due to the great workload and complex knowledge it requires. For these reasons, in general, the CAD model may come from suppliers who don’t have the qualification to do the structural analysis and vice versa, CAE models are used by structuralists who don’t have all the engineering knowledge needed to create manufacturing drawings. Moreover, it is known that, in order to make manufacturing drawings, in CAD drawings some gaps are left to be filled by weld seams or other techniques. Such a CAD model is not functional from the point of view of structural analysis. Another problem that generates difficulties in obtaining CAD models is that CAD model providers can work in a drawing program (often older and less performing) while the team performing structural analysis needs the CAD model appropriate to another program.

Considering these obstacles to the direct use of the original designer's CAD model in the structural analysis, a first part of the article is dedicated to transforming the original CAD model presented in figure1 into the CAE model undergoing structural analysis in the CAD-CAE SolidWorks program.

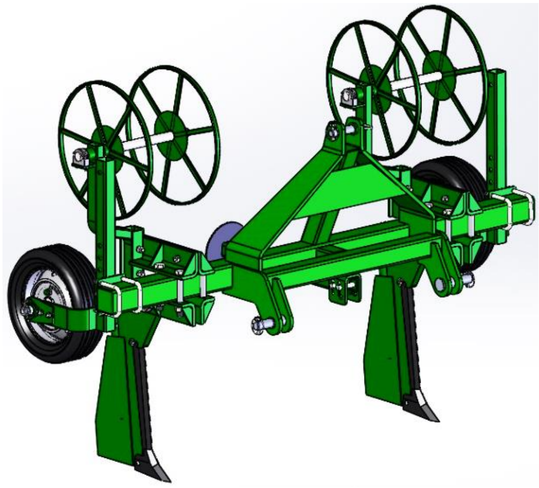

Fig. 1. CAD model of the structure in the usual form for SolidWorks program

The second part of the article presents the elementary results of the structure elastic-static analysis as proof that the transformation was correct. The fact that the results of the structural model are correct, so the results of the structural analysis are correct, can only be found experimentally. For the time being, as we don't have experimental results, we rely on the fact that the structure has worked in difficult conditions without the occurrence of deficiencies or damages. Experiments will be done after we have accumulated enough theoretical data to test as many of them within the same experiment. Global concerns in most of the directions that our research addresses are very common [5], [6], [7], [8], [9].

2. Material and method

2.1 Converting SolidWorks CAD model into simplified SolidWorks CAE model

CAD conversion to CAE resulted in an assembly that could not be used for structural analysis. To solve this impediment we isolated each benchmark, we revealed each piece and assembled it until it reached its final shape. After making the final assembly, with all its parts, it is necessary to check the existence of interferences in the structure, fig. 2, because the presence of interference (overlap or gap) can prevent the analysis program from running, or, even worse, make it run using wrong results.

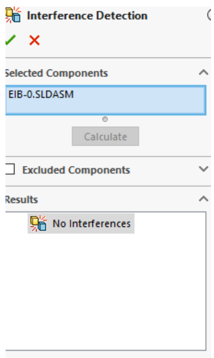

Fig. 2. Checking the interferences before starting structural analysis

2.2 CAE model structural analysis

The CAE model is simplified, fig.3. This model introduced in the structural analysis does not contain the rear superstructure of the machine or some small subassemblies. Not all subassemblies are important.

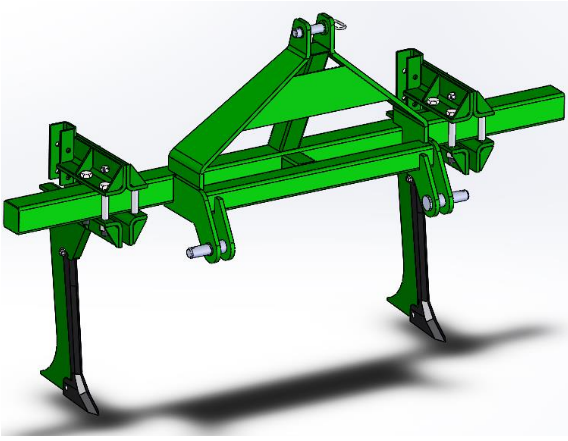

Fig. 3. The simplified CAD model subjected to finite element analysis

2.3 Fixing conditions (Structure bearing)

The structure is borne in three points by the tractor attachment system, Figure 4. The attachment to the tractor is (exaggeratedly) made by inserting (cancelling all degrees of freedom on the contact surfaces between the tractor and equipment attachment elements).

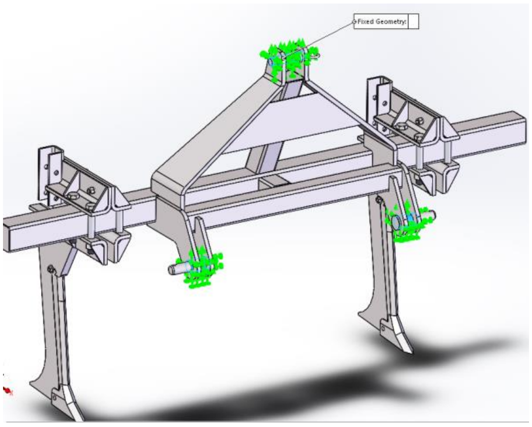

Fig. 4. Structure bearing

2.4 Structure loading

In this article, we study the response of the structure only for the normal maximum workload. The total force applied to the projection of working parts on the normal plane to the travel direction was calculated using the method of [10], [11], [12].

$$F = ka_0b_0 + \varepsilon a_0b_0v^2 \quad (1)$$

where the sizes with index 0 correspond to the working parts, (corresponding to the working depth, up to the working parts level). In (1) F_0 are the resistance forces of the soil at the action of the two parts of the working body, a_0, b_0, are the working depth and width of the working body's respective parts, while k_0, ε_0, are soil specific resistances to deformation and soil resistance to deformation coefficients due to the working speed. The working speed has been noted with *v*. In the example considered with depth of work at 40 cm, we used the following values: $a_0 b_0 = 0{,}021\ \text{m}^2$, k_0= 100000 Pa, ε= 2200 kg/m^3, v= 4 km/h. The calculated force was applied to the structure according to the graphical representation in Fig. 5.

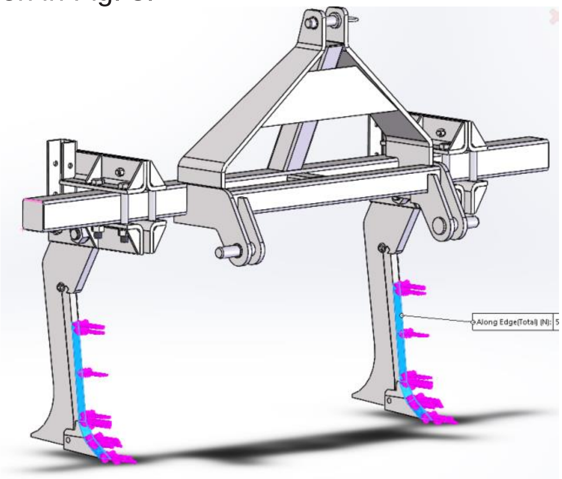

Fig. 5. Loads application (forces)

To perform linear-elastic static analysis, the global contact command was applied. This condition applied by the finite element analyser eliminates any kind of clearance, creating stress conditions corresponding to a more rigid structure than the real one. Thus, tensions will be higher than in reality, and relative displacements (deformations) are expected to have lower values than in reality. The discretization of the structure can be seen in Figure 6.

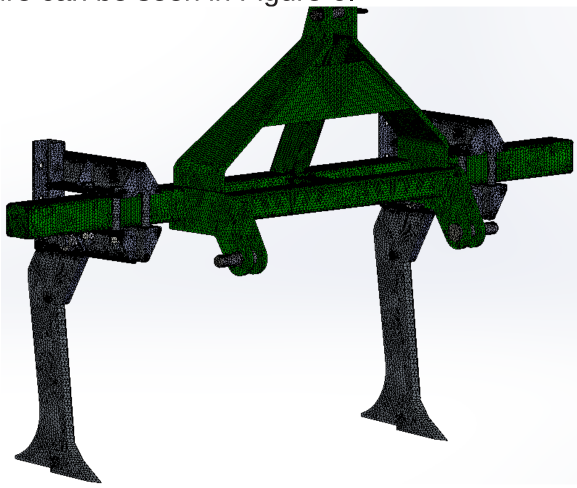

Fig. 6. Structure discretization: Projection of finite elements on the structure border

The materials used for the components of the analyses structure are shown in Figure 7 together with the respective properties. For the pipes, S275JR was used, S355 was used for the plate parts and 16MnCr5 was used for the working parts.

Property	Value	Units
Elastic modulus	2.100000031e+011	N/m^2
Poisson's ratio	0.28	N/A
Shear modulus	7.9e+010	N/m^2
Mass density	7800	kg/m^3
Tensile strength	410000000	N/m^2
Compressive Strength in X		N/m^2
Yield strength	275000000	N/m^2
Thermal expansion coefficient	1.1e-005	/K
Thermal conductivity	14	W/(m·K)
Specific heat	440	J/(kg·K)
Material Damping Ratio		N/A

a)

Property	Value	Units
Elastic modulus	2.100000031e+011	N/m^2
Poisson's ratio	0.28	N/A
Shear modulus	7.9e+010	N/m^2
Mass density	7800	kg/m^3
Tensile strength	450000000	N/m^2
Compressive Strength in X		N/m^2
Yield strength	275000000	N/m^2
Thermal expansion coefficient	1.1e-005	/K
Thermal conductivity	14	W/(m·K)
Specific heat	440	J/(kg·K)

b)

Property	Value	Units
Elastic modulus	2.100000031e+011	N/m^2
Poisson's ratio	0.28	N/A
Shear modulus	7.9e+010	N/m^2
Mass density	7800	kg/m^3
Tensile strength	800000000	N/m^2
Compressive Strength in X		N/m^2
Yield strength	590593984	N/m^2
Thermal expansion coefficient	1.1e-005	/K
Thermal conductivity	14	W/(m·K)
Specific heat	440	J/(kg·K)

c)

Fig. 7. Material properties: a) S75JR, b) S355 and c) 16MnCr5

3. Results

The main results of the static linear-elastic structural analysis are: the values of the reactions in the holders, vector field distribution of the relative - resultant displacement in the structure, tensor fields' distribution of the specific deformation and the Cauchy stress tensor in the same structure. Also, an important result for the structure safety is the distribution of the safety factor.
Table 1 shows the values of the resultant forces components, which are also found in the values of the reaction forces (in the three bearing areas).

Table 1: Resultant Forces

Components	X	Y	Z	Resultant
Reaction force(N)	5677.45	-0.230323	0.29408	5677.45
Reaction Moment(N·m)	0	0	0	0

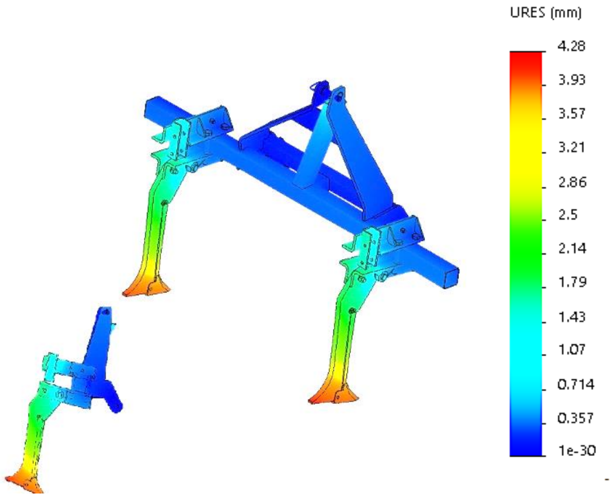

Fig. 8. Distribution of the relative displacement field values resulting on the structure border

Figure 8 graphically represents the distribution maps of the relative displacement field values on the structure border. It is noticed that the maximum value (about 4 mm) is located at the back of the structure. This maximum value can be exceeded if we take into account the clearances of the structure and of the connection system between the equipment and the tractor. Increasing the movement, in the conditions of the considered stress, admitting the clearances, contributes to the relaxation of the structure and consequently to the increase of the safety factor. However, exaggerated clearances generally lead to more or less premature wear.

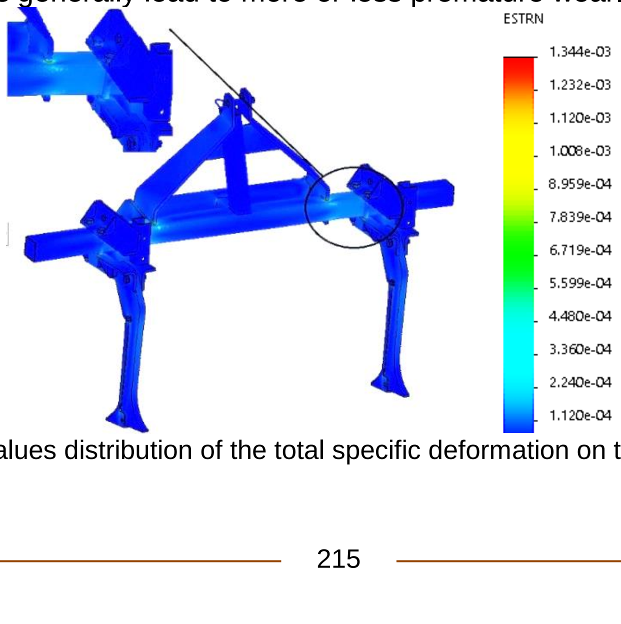

Fig. 9. Field values distribution of the total specific deformation on the structure border

In figure 9, the distribution of the total specific deformation values is graphically represented by color map. The maximum stress area is also indicated in detail. Due to the fact that we are working in the elastic-linear field, the maximum tension will be located in the same area as the maximum specific deformation. The maximum equivalent tension is graphically indicated in the same way in Figure 10.

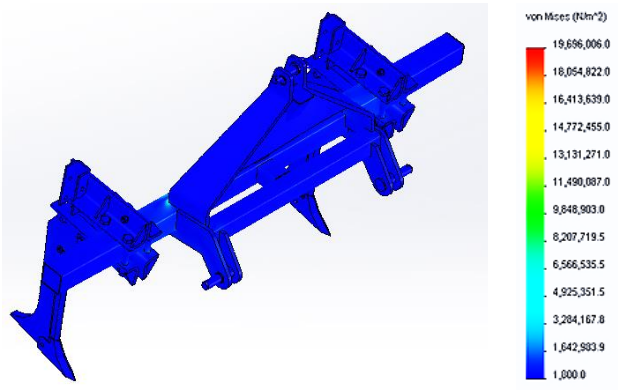

Fig. 10. Representation of the equivalent tension distribution on the structure border

Finally, Figure 11 shows the graphical representation of the safety factor distribution in the structure.

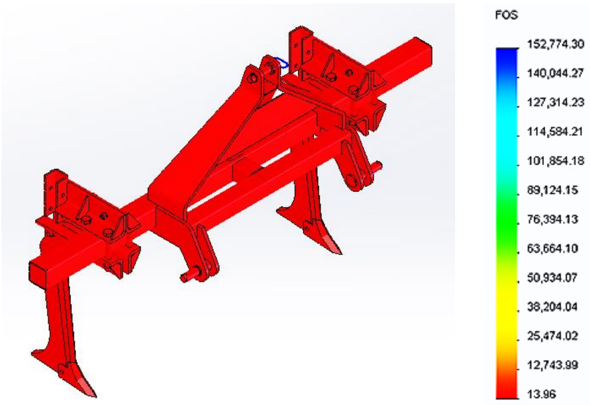

Fig. 11. Safety factor distribution in the structure border

The minimum safety coefficient value is 13.96. For agricultural machinery destined to soil works, the usual safety coefficient values are between 1.8 and 2.2. Therefore, this machine is either much oversized, or it works under much tougher conditions. The latter may appear either due to use under improper conditions or due to accidents (impact with hard rocks or roots in soil).

4. Conclusions

Following this first structural study on the drip tape injection equipment, several important conclusions can be drawn for further investigations.

For a normal load, calculated according to the criteria outlined in the paper, the load-bearing structure of the equipment is overestimated, leaving aside possible accidents in the soil (hard bodies) or the use under improper conditions.

Considering the maximum values of equivalent tension, there are no risks of structure material failure. Also, the maximum relative displacement values guarantee that deviations from working parameters dictated by agrotechnical requirements (working depth, in particular) are negligible, at least regarding the essential part of the equipment work.

The high value of the safety coefficient (13.96), in relation to its usual values in the practice of designing and manufacturing agricultural machinery for soil works, shows that there is an important potential for optimizing this machine. Since the equipment could be used on a land that has not been tilled for five to ten years, there is the possibility of accepting a coefficient of up to 7 - 8; therefore, it would be the case for a substantial optimization study.

Acknowledgments

This work was supported by a grant of the Romanian Ministry of Research and Innovation CCDI - UEFISCDI, Project INNOVATIVE TECHNOLOGIES FOR IRRIGATION OF AGRICULTURAL CROPS IN ARID, SEMIARID AND SUBHUMID-DRY CLIMATE, project number PN-III-P1-1.2-PCCDI-2017-0254, Contract no. 27PCCDI / 2018, within PNCDI III.

References

[1] Ayars, J.E., C.J. Phene, R.B. Hutmacher, K.R. Davis, R.A. Schonemana, S.S. Vail, and R.M. Mead. "Subsurface drip irrigation of row crops: a review of 15 years of research at the Water Management Research Laboratory." *Agricultural Water Management*, Volume 42, Issue 1, September 1999.
[2] NETAFIM USA. *Manual for Corn Production Using Subsurface Drip Irrigation*. https://www.netafimusa.com/.
[3] Camp, C.R. and F.R. Lamm, "Irrigation systems, subsurface drip". *Encyclopedia of Water Science* (2003), pp. 560-564.
[4] Enciso, Juan. "Installing a Subsurface Drip Irrigation System for Row Crops". Texas A&M AgriLife Extension Service. AgriLife Extension.tamu.edu.
[5] Cardei, Petru, A. Meca, and Georgi Kostadinov. “Working regimes of the agricultural machines designed to soil tillage: From optimization to fundamentals (1).” *INMATEH*, vol. 37, No. 2/2012, pp.13 – 20.
[6] Cardei, Petru, and Georgi Kostadinov. “Working regimes of the agricultural machines designed to soil tillage: From optimization to fundamentals (2).” *INMATEH*, vol. 37, No. 2/2012, pp. 21 – 28.
[7] Nagy, M., Petru Cardei, C. Cota, and L. Fechete. “Method of estimating the soil resistance force to soil working machine parts with applications to the optimization of working regimes of machines used in horticulture.” *INMATEH*, vol. 35, No. 3/2011, pp.27 – 32.
[8] Kadam, Arjun, and Narendra Chhapkhane, “Design and analysis of subsoiler.” *International Journal of Modern Trends in Engineering and Science*, ISSN: 2348-3221, pp. 11-14.
[9] Gheorghe, G., C. Persu, M. Matache, M. Mateescu, and D. Cujbescu. “Finite element method use in the calculation and optimization of the active parts of mulch films applying equipment.” *Agricultural and mechanical engineering*, ISSN 2537 – 3773, pp.629-634
[10] Letosnev, M. N. *Agricultural Machines*, Agrosilvica State Publishing House, Bucharest, 1959.
[11] Krasnicenko, A.V. *Agricultural Machinery manufacturer manual*, volume 2, Technical Publishing House, Bucharest, 1964.
[12] Sandru, A., S. Popescu, I. Cristea, and V. Neculaiasa. *Agricultural machinery exploitation*, Didactic and Pedagogical Publishing House, Bucharest, 1983.